The Journal of Physical Chemistry Letters

Two Spin-State Reactivity in the Activation and Cleavage of CO_2 by $[ReO_2]^-$.

Journal:	*The Journal of Physical Chemistry Letters*
Manuscript ID	jz-2016-007546.R1
Manuscript Type:	Letter
Date Submitted by the Author:	n/a
Complete List of Authors:	Canale, Valentino; University "G.d\'Annunzio", Department of Engineering and Geology Robinson, Robert; University of Tasmania, School of Physical Sciences - Chemistry Zavras, Athanasios; School of chemistry, Bio21 Institute Khairallah, George; Bio21 Institute, Chemistry d'Alessandro, Nicola; University "G.d'Annunzio", Department of Engineering and Geology Yates, Brian; University of Tasmania, School of Chemistry O'Hair, Richard; Inst of Molecular Science/ Biotechnology, School of Chemistry

Version: 5 May 2016
Submitted to: *J. Phys. Chem. Lett.*

Two Spin-state Reactivity in the Activation and Cleavage of CO_2 by $[ReO_2]^-$

Valentino Canale,[a-c,‡] Robert Robinson Jr.,[d,‡] Athanasios Zavras,[a,b] George N. Khairallah,[a,b] Nicola d'Alessandro,[c] Brian F. Yates,*[,d] and Richard A. J. O'Hair*[,a,b]

[a]School of Chemistry and Bio21 Molecular Science and Biotechnology Institute, University of Melbourne, 30 Flemington Rd, Parkville, Victoria 3010 (Australia). Fax: (+)61 3 9347 8124; E-mail: rohair@unimelb.edu.au

[b]ARC Centre of Excellence for Free Radical Chemistry and Biotechnology.

[c]Department of Engineering and Geology (INGEO), "G. d'Annunzio" University of Chieti and Pescara, Viale Pindaro, 42, I-65127 Pescara, Italy

[d]School of Physical Sciences - Chemistry, University of Tasmania, Private Bag 75, Hobart, Tasmania 7001, Australia

[‡]These authors contributed equally to the work.

ABSTRACT:

The rhenium dioxide anion $[ReO_2]^-$ reacts with carbon dioxide in a linear ion trap mass spectrometer to produce $[ReO_3]^-$ corresponding to activation and cleavage of a C-O bond. Isotope labeling experiments using $[Re^{18}O_2]^-$ reveal that $^{18}O/^{16}O$

scrambling does not occur prior to cleavage of the C-O bond. DFT calculations were performed to examine the mechanism for this oxygen atom abstraction reaction. Since the spins of the ground states are different for the reactant and product ions ($^3[ReO_2]^-$ versus $^1[ReO_3]^-$), both reaction surfaces were examined in detail and multiple $[O_2Re\text{-}CO_2]^-$ intermediates and transition structures were located as well as minimum energy crossing points were calculated. The computational results show that the intermediate $[O_2Re(\eta^2\text{-}C,O\text{-}CO_2)]^-$ species most likely initiates C-O bond activation and cleavage. The stronger binding affinity of CO_2 within this species and the greater instabilities of other $[O_2Re\text{-}CO_2)]^-$ intermediates are significant enough that oxygen atom exchange is avoided.

TOC GRAPHIC:

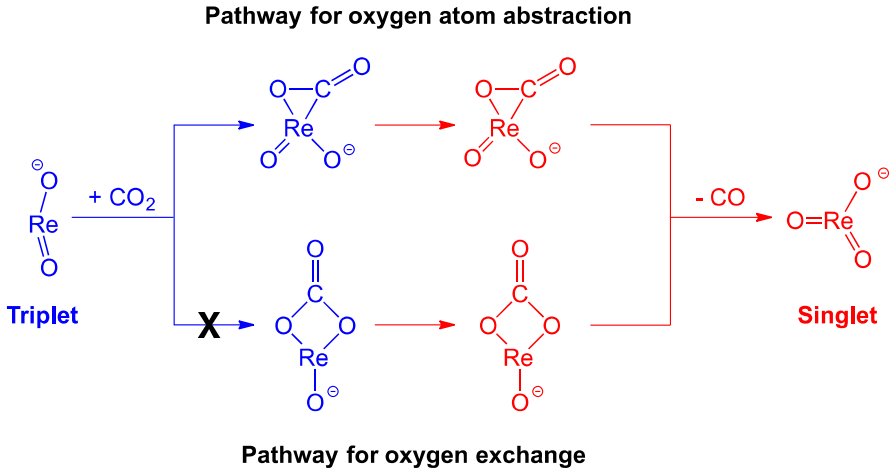

MAIN TEXT:

There is intense interest in finding ways to use transition metal complexes to activate strong bonds in simple diatomic and triatomic molecules, with applications in areas such as artificial nitrogen fixation and carbon dioxide utilization [1]. While rhenium

oxo compounds have found applications in organic synthesis [2,3] and in biomass conversion [4], their role in transforming simple diatomic and triatomic molecules has been largely neglected. This is surprising since rhenium can support a number of oxidation states, allowing rhenium oxo compounds to either behave as oxygen atom donors or acceptors and thus oxidize or reduce substrates. Examples are methylrhenium trioxide, which acts as a catalyst to oxidize alkenes to epoxides [5] and methylrhenium dioxide, which acts as a catalyst to reduce epoxides to alkenes [6]. We recently examined the gas-phase reactivity of the rhenium oxide anions, $[ReO_x]^-$ (x = 2 – 4) towards the organic substrates: methane, ethylene, methanol and acetic acid. Only $[ReO_2]^-$ and acetic acid reacted with each other, with $[ReO_3]^-$ being one of the products formed [7]. The observation of this formal oxygen atom abstraction reaction occurring at near room temperature has prompted us to use a combination of gas-phase experiments and computational chemistry to examine whether CO_2 can be activated and cleaved in its reactions with $[ReO_2]^-$. Such a reaction is of both fundamental interest as it may involve two spin-state reactivity [8] in order to proceed from the $[ReO_2]^-$ triplet ground state to the $[ReO_3]^-$ singlet ground state [9] as well as for potential applications in developing methods for the chemical conversion and utilization of the greenhouse gas, carbon dioxide [10-18]. In particular, room temperature carbon dioxide activation remains challenging, but critical.

$[ReO_2]^-$ reacts cleanly (Figure 1a) with CO_2 in a linear ion trap mass spectrometer via oxygen atom abstraction to produce $[ReO_3]^-$ (Figure 1, eq. 1). In contrast, $[ReO_3]^-$ and $[ReO_4]^-$ are unreactive towards CO_2 under the same experimental conditions. When $[Re^{18}O_2]^-$ reacts with CO_2, $[Re^{18}O_2{}^{16}O]^-$ is almost exclusively formed (Figure 1b), highlighting that oxygen atom scrambling is not an important process on the potential

energy surface associated with the oxygen atom abstraction reaction [19,20]. The rate of reaction, determined from the decay of $[ReO_2]^-$, was found to be 1.9 (±0.1) x 10^{-12} $cm^3.molecules^{-1}.s^{-1}$, which corresponds to a reaction efficiency of 0.3%.

$$\underset{m/z\ 219}{[ReO_2]^-} + CO_2 \rightarrow \underset{m/z\ 235}{[ReO_3]^-} + CO \qquad (1)$$

Figure 1. Gas-phase ion-molecule reactions of CO_2 with: **(a)** $[ReO_2]^-$ (reaction time = 60 ms) **(b)** $[Re^{18}O_2]^-$ (reaction time = 100 ms). Concentration of CO_2 was 3.86 x 10^{12} molecules.cm^{-3}.

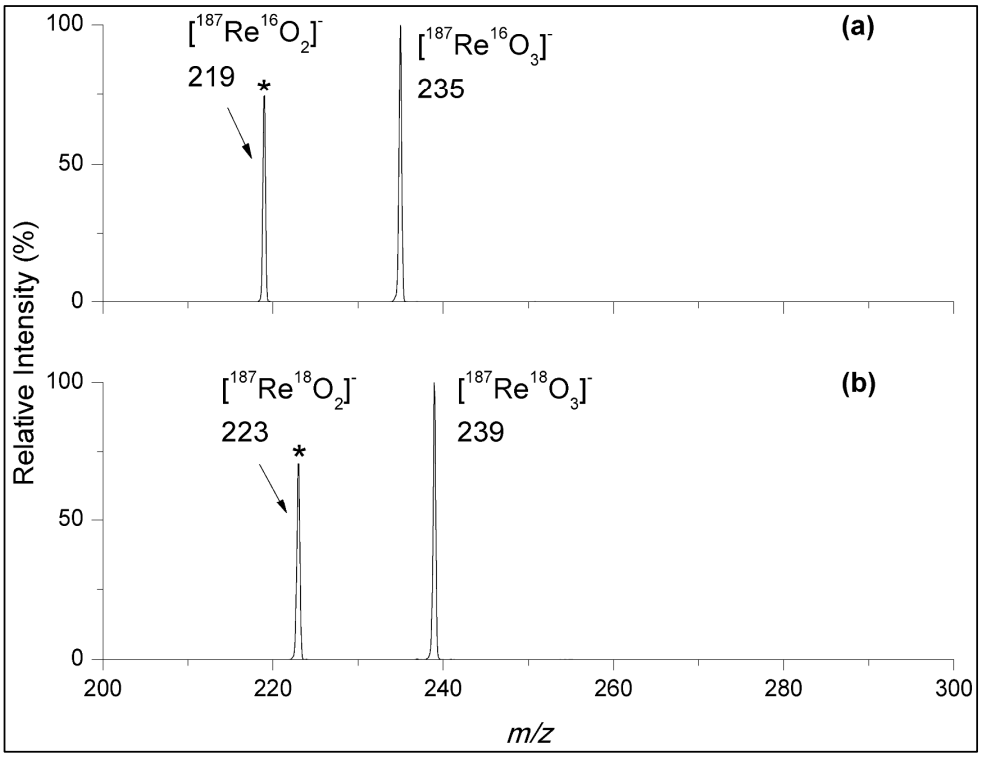

In order to gain insights into the sluggish nature of the reaction of $[ReO_2]^-$ with CO_2 and to offer a rationale for the lack of oxygen atom exchange, we turned to the use of DFT calculations to examine the mechanistic details of this reaction [21]. In order to

find a suitable level of theory to calculate the reaction thermochemistry, benchmarking studies were carried out on the electron affinities (EAs) of ReO_2 and ReO_3 and the bond lengths for quartet-ReO_2 and triplet-$[ReO_2]^-$ (Supporting Information Tables S1, S2 and S3) [22]. The B3LYP/BS2//B3LYP/BS1 level of theory was used for all subsequent calculations since it gave good agreement with the experimentally determined EAs and there was acceptable agreement with the bond lengths calculated using various levels of theory and basis sets. $^3[ReO_2]^-$ is calculated to be 67.4 kJ.mol^{-1} more stable than $^1[ReO_2]^-$ (Supporting Information Table S4), while $^1[ReO_3]^-$ is calculated to be 143.2 kJ.mol^{-1} more stable than $^3[ReO_3]^-$ (Figure 2). This predicted change in the ground state from $[ReO_2]^-$ to $[ReO_3]^-$ is consistent with a previous study [9]. Reaction of $^3[ReO_2]^-$ with CO_2 is calculated to be exoergic by 38.0 kJ.mol^{-1} when forming $^3[ReO_3]^-$ and CO and exoergic by 181.2 kJ.mol^{-1} for the formation of $^1[ReO_3]^-$ and CO. Since the latter products are considerably more stable, this suggests that this reaction may proceed via a two spin-state reactivity involving a switch from the triplet to the singlet surface. Both reaction surfaces were examined in detail and multiple $[O_2Re\text{-}CO_2]^-$ intermediates and transition structures were located (Supporting Information Figure S1).

An examination of the simplified reaction surfaces (Figure 2), reveals the following features: (I) The oxygen atom abstraction reaction (eq. 1) can either occur on the triplet surface or via two spin-state reactivity. The latter are not only energetically preferred overall, but also avoid either of the higher energy transition states **TSB3_T** or **TSB8_T** being formed. (II) Two pathways to intersystem crossing from the triplet to the singlet surface were identified via minimum energy crossing points (MECPs): (*i*) an "early" crossing from triplet **3_T** to singlet **3_S** via **3_MECP** and then via bond

breaking transition structure **TSB3_S** to products; or (*ii*) a "later" crossing requiring traversing breaking transition structure **TSB3_T** from triplets **3_T** to **8_T** via **8_MECP** followed by crossing to singlet **8_S** that decomposes immediately to products. Even though other $[O_2Re\text{-}CO_2]^-$ intermediates are capable of undergoing oxygen atom abstraction reactions, their relative stabilities lie above that of the breaking transition structure **TSB3_T** (Figure 2). The only exceptions are triplet **7_T** and singlet $[O_2Re(\eta^2\text{-}O,O\text{-}CO_2)]^-$ **6_S**, which both have significant endoergic barriers (>67 kJ.mol^{-1}) for formation (Supporting Information Figure S1). The *early* pathway (from **3_T** to **3_S)** is calculated to be 13.4 kJ.mol^{-1} less energetic for intersystem crossing than the *later* pathway (from **8_T** to **8_S**). In contrast, the *later* pathway (via breaking transition structure **TSB3_T**) is calculated to be 63.0 kJ.mol^{-1} less energetic for cleavage of a C-O bond than the *early* pathway (via breaking transition structure **TSB3_S**). On the basis of these computational results, we predict that these two different pathways are likely to be competitive. (III) Although a quantitative modeling of the overall rate of the oxygen atom abstraction reaction from the DFT calculated surfaces is beyond the scope of this work [23], the rate-determining step is likely to be either **2-P** or **3-P**. The sluggish nature for the reaction of $[ReO_2]^-$ with CO_2 can be attributed to a thermodynamic bottleneck at the entrance channel, which is key to initiate the oxygen atom abstraction process. There is a slightly unfavorable preliminary interaction between $^3[ReO_2]^-$ and CO_2 to form either **2-P** or **3-P**. Thus most collisions between $[ReO_2]^-$ with CO_2 will result in dissociation back to reactants, consistent with the observed low reaction efficiency of 0.3%.

Figure 2. Calculated low-energy reaction pathways for the two spin-state reactivity of $[ReO_2]^-$ with CO_2. A more complete set of calculated pathways is given in Supporting Information Figure S1. The inset shows the structures of the two key minimum energy crossing points (MECPs).

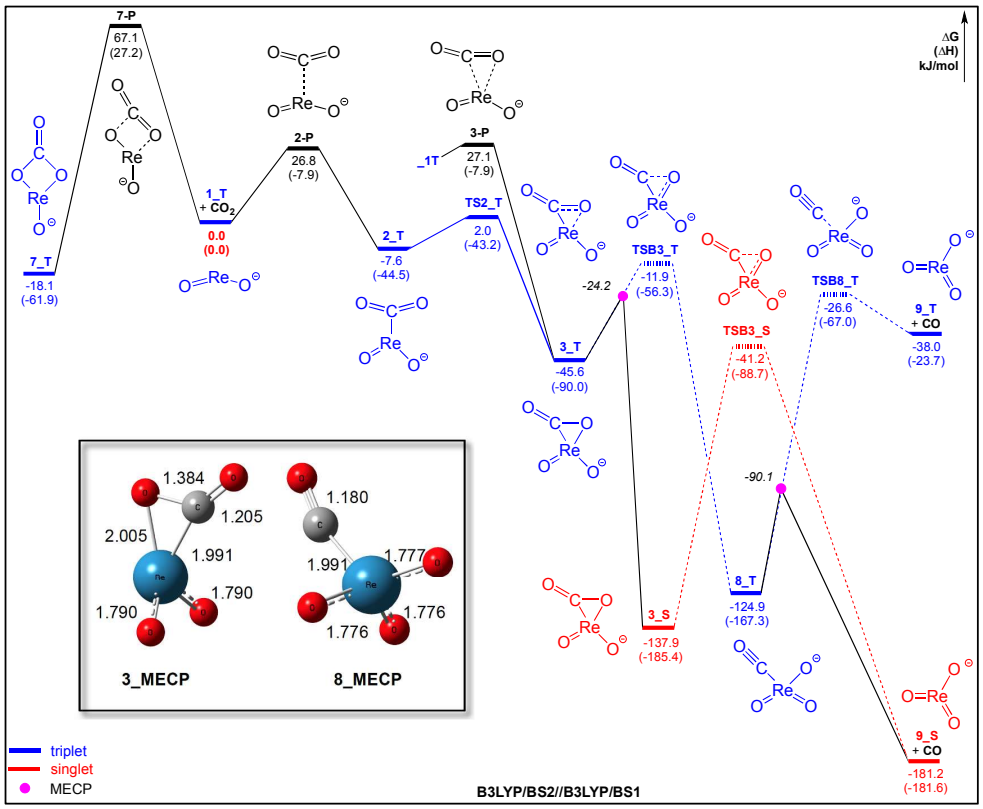

Previous studies on the gas-phase reactions of the silaformyl anion, $HSi^{18}O^-$ with CO_2 found extensive oxygen atom scrambling, where *ab initio* calculations revealed the formation of a four-membered ring as a key intermediate in this process [19,20]. The lack of a related oxygen atom scrambling process in the reaction of $[ReO_2]^-$ with CO_2 is consistent with the following salient features of the DFT calculated surface (Figure S1):

(I) The formation of triplet **3_T** and singlet **3_S** is exoergic by -45.6 and -137.9 kJ.mol^{-1}, respectively. The barrier for extrusion of CO from the three-membered ring of singlet **3_S** via breaking transition structure **TSB3_S** lies -41.2 kJ.mol^{-1} below the separated reactants, which allows for a direct pathway for oxygen atom abstraction that does not involve oxygen atom scrambling.

(II) In contrast, the formation of the four-membered ring of triplet **7_T** is less exoergic (-18.1 kJ.mol^{-1}), while the formation of singlet **7_S** is endoergic by +54.9 kJ.mol^{-1} and the barrier for extrusion of CO from singlet **7_S** via breaking transition structure **TSB7_S** lies a prohibitive +162.2 kJ.mol^{-1} above the separated reactants (Supporting Information Figure S1).

(III) The barrier to the formation of triplet **3_T** is substantially less than that for the formation of triplet **7_T** (27.1 versus 67.1 kJ.mol^{-1}), suggesting the exclusive formation of triplet **3_T** directly from the reactants.

(IV) We have been unable to locate a transition structure between triplets **3_T** and **7_T**. Thus once formed, it is unlikely that triplet **3_T** is able to interconvert with triplet **7_T**.

Overall, the DFT calculations suggest that it is not possible to either directly or indirectly access the critical four- membered ring intermediate required for oxygen scrambling.

Finally, while the observed reaction of $[ReO_2]^-$ with CO_2 is inefficient, it occurs selectively and at room temperature, which should encourage the search for rhenium oxo catalysts that can achieve the same transformation on a bulk scale.

METHOD SECTION:

Experimental

Reagents:

The following reagents were used as received: rhenium(V) chloride, $ReCl_5$ (99.9%-Re, STREM Chemicals); acetonitrile, MeCN (analytical grade, Ajax Finechem); and gaseous carbon dioxide, CO_2 (1.03% in helium, Coregas). $H_2{}^{[18]}O$ was a gift from Prof. Jonathon M. White at The University of Melbourne.

Mass Spectrometry:

Mass spectrometric experiments were conducted on a Thermo Scientific (Bremen, Germany) LTQ FT hybrid mass spectrometer consisting of a linear ion trap (LTQ) coupled to a Fourier-transform ion cyclotron resonance (FT-ICR) mass spectrometer, which has been modified to allow the study of ion-molecule reaction [24]. Under ion-molecule reaction conditions, collisions with the helium bath gas quasi-thermalizes the ions to room temperature [25].

To generate $[ReO_2]^-$, 5 mg of rhenium(V) chloride was dissolved in 500 µL of H_2O, then 3 mg of silver oxide was added and the resultant mixture was shaken for 1 min to facilitate dissolution. This mixture was diluted to a final concentration of 50 µL in acetonitrile and injected into the ESI source. Typical ESI conditions used were: spray voltage, 3.0-5.0 kV, capillary temperature, 250-270°C, nitrogen sheath pressure, 15-20 (arbitrary units), and capillary voltage/tube lens offset, were tuned to maximize the desired peak. The injection time was set using the AGC (automatic gain control) function. To generate $[Re^{[18]}O_2]^-$, 5 mg of rhenium(V) chloride was dissolved in 500 µL of $H_2{}^{[18]}O$, then diluted in acetonitrile and injected into the ESI source.

The most abundant rhenium isotope, ^{187}Re, of $[ReO_2]^-$ was mass selected using a 1–2 Th window. The ion-molecule-reactions conditions were: activation energy 0%; Q of 0.25, and the reaction time was varied between 10 ms and 10000 ms prior to ejection from the ion-trap for detection. Under pseudo-first order conditions, the ion-molecule reactions of $[ReO_2]^-$ with excess CO_2 were monitored. A total of 10 data sets for product ion intensity versus various reaction times (10–100 ms) were recorded and these were averaged (see Supplementary Material Figure S2). Theoretical rates for the reaction were calculated with the program COLRATE [26] using the Average Dipole Orientation (ADO) theory of Su and Bowers [27].

High-resolution mass spectra were acquired in the FTICR to confirm the identity of the precursor and product ions observed, as described previously [28].

Computational

DFT calculations in the gas-phase were performed to examine the structure and the stability of rhenium containing anions and to estimate the energetics of their reactions using the Gaussian09 [29] package. Based upon our benchmarking studies (supplementary material), full geometry optimizations at standard conditions (298.15 K and 1 atm) were carried out using the B3LYP [30-32] functional together with a mixed basis set consisting of the SDD basis set [33] with effective core potential (ECP) for rhenium combined with the 6-31G(d) basis set for all other atoms (C and O), which we designate hereafter as B3LYP/BS1. Vibrational frequency analysis was carried out at the same level of theory in order to confirm that the full geometry optimizations are local minima and transition structures. IRC [34,35] calculations were used to confirm the connectivity between transition structures and minima.

Intersystem crossings between spin-states were located at minimum energy crossing points (MECPs) using the code of Harvey *et al* [36] and are reported uncorrected due to the absence of stationary points. To further refine the energies obtained from the B3LYP/BS1 calculations, we carried out single-point energy (SPE) calculations on all of the geometry optimizations using both the B3LYP and M06 [37-40] functionals together with a mixed basis set consisting of the quadruple-ζ valence def2-QZVP [41] with ECP for rhenium combined with the 6-311+G(2d,p) basis set for all other atoms (C and O), which we designate hereafter as B3LYP/BS2 and M06/BS2, respectively. All reported energies are calculated from adding the SPEs and the corresponding thermal correction to the Gibbs free energy ($E_{reported} = E_{SPE} + E_{Gibb}$), unless noted otherwise.

The nomenclature used in this letter is as follows: (i) **N** (numbers) represent minima and **TS** represent conversion transition structures; (ii) spin-states are denoted by **_S** (singlet) and **_T** (triplet); (iii) breaking transition structures by **TSB**; and (iv) preliminary interactions by **-P**.

ASSOCIATED CONTENT:

Supporting Information

Additional supporting information, which includes: mass spectra showing the gas-phase ion-molecule reactions of CO_2 with $[ReO_2]^-$ and $[Re^{18}O_2]^-$; benchmarking studies on the electron affinities of ReO_2 and ReO_3; complete calculated reaction pathway for the two spin-state reactivity of $[ReO_2]^-$ with CO_2; Cartesian coordinates and total energies for all calculated structures; a full citation of ref. 29 may be found in the online version of this article.

AUTHOR INFORMATION:

Corresponding Author

*E-mail: Brian.Yates@utas.edu.au and rohair@unimelb.edu.au.

Notes

The authors declare no competing financial interest.

ACKNOWLEDGMENTS:

We thank the ARC for financial support via the ARC Centre of Excellence for Free Radical Chemistry and Biotechnology (CE0561607), the award of an ARF to GNK (DP1096134), and Discovery Projects to BFY (DP120101937) and RAJO (DP150101388). The authors gratefully acknowledge the generous allocation of computing time from the Melbourne University high performance computing Facility (Edward), from the Tasmanian Partnership for Advanced Computing (Katabatic), and from the National Computing Infrastructure (Raijin). VC thanks the University G.d'Annunzio of Chieti-Pescara and the Italian Ministry of Education, University and Research for financial support (Fondo Sostegno Giovani). We thank Prof Jonathon White for a gift of $H_2{}^{[18]}O$ and Prof Helmut Schwarz for a preprint of ref. 13.

REFERENCES AND FOOTNOTES:

(1) Lu, C. C.; Meyer, K. Small-molecule activation by reactive metal complexes. *Eur. J. Inorg. Chem.*, **2013**, 3731-3732.

(2) Romao, C. C.; Kuhn, F. E.; Hermann, W. A. Rhenium(VII) oxo and imido complexes: Synthesis, structures, and applications. *Chem. Rev.* **1997**, *97*, 3197-3246.

(3) Bellemin-Laponnaz, S. Perrhenate esters in new catalytic reactions. *ChemCatChem.* **2009**, *1*, 357-362.

(4) Korstanje, T. J.; Gebbink, R. J. M. K. Catalytic oxidation and deoxygenation of renewables with rhenium complexes. *Top. Organomet. Chem.* **2012**, *39*, 129-174.

(5) Hudson, A. Methyltrioxorhenium in *Encyclopedia of Reagents for Organic Synthesis*; John Wiley & Sons: New York, USA; **2002**.

(6) Harms, R. G.; Herrmann, W. A.; Kühn, F. E. Organorhenium dioxides as oxygen transfer systems: Synthesis, reactivity, and applications. *Coord. Chem. Rev.* **2015**, *296*, 1–23.

(7) Canale, V.; Zavras, A.; Khairallah, G. N.; d'Alessandro, N.; O'Hair, R. A. J. Gas phase reactions of the rhenium oxide anions, $[ReO_x]^-$ (x = 2 – 4) with the neutral substrates methane, ethene, methanol and acetic acid. *Eur. J. Mass Spectrom.* **2015**, *21*, 557–568.

(8) Schroeder, D.; Shaik, S.; Schwarz, H. Two-state reactivity as a new concept in organometallic chemistry. *Acc. Chem. Res.* **2000**, *33*, 139-145.

(9) Zhou, M.; Citra, A.; Liang, B.; Andrews, L. Infrared spectra and density functional calculations of MO_2, MO_3, $(O_2)MO_2$, MO_4, MO_2^- (M = Re, Ru, Os) and ReO_3^-, ReO_4^- in solid neon and argon, *J. Phys. Chem. A*. **2000**, *104*, 3457-3465.

(10) Sakakura, T.; Choi, J. -C.; Yasuda, H. Transformation of carbon dioxide. *Chem. Rev.* **2007**, *107*, 2365–2387.

(11) Cokoja, M.; Bruckmeier, C.; Rieger, B.; Herrmann, W. A.; Kühn, F. E. Transformation of carbon dioxide with homogeneous transition-metal catalysts: A molecular solution to a global challenge? *Angew. Chem. Int. Ed.* **2011**, *50,* 8510–8537.

(12) Liu, Q.; Wu, L.; Jackstel, R.; Beller, M. Using carbon dioxide as a building block in organic synthesis, *Nature Comm.* **2015**, 5933.

(13) For a review on the gas-phase reactions of CO_2 with metal ions and metal containing ions using mass spectrometry based techniques see: Schwarz, H. Metal-

mediated activation of carbon dioxide in the gas phase: Mechanistic insight derived from a combined experimental/computational approach. *Coord. Chem. Rev.* **2016**, DOI: 10.1016/j.ccr.2016.03.009.

(14) Brookes, N. J.; Ariafard, A.; Stranger, R.; Yates, B. F. Cleavage of carbon dioxide by an iridium-supported Fischer carbene. A DFT investigation, *J. Am. Chem. Soc.* **2009**, *131*, 5800–5808.

(15) Portenkirchner, E.; Kianfar, E.; Sariciftci, N. S.; Knor, G. Electrocatalytic reduction of carbon dioxide to carbon monoxide by a polymerized film of an alkynyl-substituted rhenium(I) complex. *ChemSusChem*. **2014**, *7*, 1790–1796.

(16) A number of rhenium photocatalysts have been developed for the reduction of CO_2. See for example: Walter, D.; Ruben, M.; Rau, S., Carbon dioxide and metal centres: from reactions inspired by nature to reactions in compressed carbon dioxide as solvent. *Coord. Chem. Rev.* **1999**, *182*, 67-100.

(17) Re^+ only undergoes a slow clustering reaction with CO_2: Koyanagi, G. K.; Bohme, D. K. Gas-phase reactions of carbon dioxide with atomic transition-metal and main-group cations: Room-temperature kinetics and periodicities in reactivity. *J. Phys. Chem. A*. **2006**, *110*, 1232–1241.

(18) Laser-ablated rhenium atoms react with CO_2 upon co-condensation in excess argon at 7 K and neon at 4 K to give the neutral products [OReCO], [O_2ReCO], [ORe$(CO)_2$] and [O_2Re$(CO)_2$] and the anionic species $[OReCO]^-$ and $[ORe(CO)_2]^-$: Liang, B. Y.; Andrews, L. Reactions of laser-ablated rhenium atoms with carbon dioxide: Matrix infrared spectra and density functional calculations on OReCO, O_2ReCO, ORe$(CO)_2$, O_2Re$(CO)_2$, $OReCO^-$, and $ORe(CO)_2^-$. *J. Phys. Chem. A*. **2002**, *106*, 595–602.

(19) Gronert, S.; O'Hair, R. A. J.; Prodnuk, S.; Sülzle, D.; Damrauer, R.; DePuy, C. H. Gas phase chemistry of the silaformyl anion, $HSiO^-$. *J. Am. Chem. Soc.* **1990**, *112*, 997-1003.

(20) Shimizu, H.; Gordon, M. S.; Damrauer, R.; O'Hair, R. A. J. Potential energy surface of the reaction of the silaformyl anion and CO_2. *Organometallics*. **1995**, *14*, 2664-2671.

(21) For a review of theoretical studies of the reactions of transition metals with CO_2, see: Fan, T.; Chen, X.; Lin, Z. Theoretical studies of reactions of carbon dioxide mediated and catalysed by transition metal complexes, *Chem. Commun.* **2012**, *48*, 10808-10828.

(22) Pramann, A.; Rademann, K. Photoelectron spectroscopy of ReO_2^- and ReO_3^-. *Chem. Phys. Lett.* **2001**, *343*, 99-104.

(23) Using RRKM modeling to estimate the overall rate of reaction from the DFT calculated surface of a multistep reaction remains a major challenge. This is due to the fact that even in systems where two state reactivity is not possible (see for example: Khairallah, G. N.; da Silva, G. R.; O'Hair, R. A. J. Molecular Salt Effects in the Gas Phase: Tuning the Kinetic Basicity of $[HCCLiCl]^-$ and $[HCCMgCl_2]^-$ by LiCl and $MgCl_2$. *Angew. Chem. Int. Ed*., **2014**, *53*, 10979–10983), small differences in barrier heights can result in rates that are different in orders of magnitude. Due to the fact O atom abstraction may involve two-state reactivity, a theoretical estimate of the overall rate of reaction further magnifies this challenge.

(24) Donald, W. A.; McKenzie, C. J.; O'Hair, R. A. J. C–H bond activation of methanol and ethanol by a high-spin $Fe^{IV}O$ biomimetic complex. *Angew. Chem. Int. Ed*. **2011**, *50*, 8379-8383.

(25) Donald, W. A.; Khairallah, G. N.; O'Hair, R. A. J. The effective temperature of ions stored in a linear quadrupole ion trap mass spectrometer. *J. Am. Soc. Mass Spectrom.* **2013**, *24*, 811-815.

(26) Lim, K. F. *Quantum Chem. Program Exch.* **1994**, *14*, 1.

(27) Su, T.; Bowers, M. T. Ion-polar molecule collisions: The effect of ion size on ion-polar molecule rate constants; the parameterization of the average-dipole-orientation theory. *Int. J. Mass Spectrom. Ion Phys.* **1973**, *12*, 347–356.

(28) Feketeová, L.; Khairallah, G. N.; O'Hair, R. A. J. Intercluster chemistry of protonated and sodiated betaine dimers upon collision induced dissociation and electron induced dissociation. *Eur. J. Mass Spectrom.* **2008**, *14*, 107-110.

(29) Gaussian 09, revision D.01, M. J. Frisch; *et al.* Gaussian, *Inc.*: Wallingford, CT; **2010**. For complete reference see the Supporting Information.

(30) Becke, A. D. Density functional thermochemistry. III. The role of exact exchange. *J. Chem. Phys.* **1993**, *98*, 5648-5652.

(31) Miehlich, B.; Savin, A.; Stoll, H.; Preuß, H. Results obtained with the correlation energy density functionals of Becke and Lee, Yang and Parr. *Chem. Phys. Lett.* **1989**, *157*, 200-206.

(32) Lee, C. T.; Yang, W. T.; Parr, R. G. Development of the Colle-Salvetti correlation-energy formula into a functional of the electron density. *Phys. Rev. B.* **1988**, *37*, 785-789.

(33) Andrae, D.; Häußermann, U.; Dolg, M.; Stoll, H.; Preuß, H. Energy-adjusted *ab initio* pseudopotentials for the second and third row transition elements. *Theoret. Chim. Acta.* **1990**, *77*, 123-141.

(34) Fukui, K. The path of chemical reactions - the IRC approach. *Acc. Chem. Res.* **1981**, *14*, 363- 368.

(35) Fukui, K. Formulation of the reaction coordinate. *J. Phys. Chem.* **1970**, *74*, 4161- 4163.

(36) Harvey, J. N.; Aschi, M.; Schwarz, H.; Koch, W. The singlet and triplet states of phenyl cation. A hybrid approach for locating minimum energy crossing points between non-interacting potential energy surfaces. *Theor. Chem. Acc.* **1998**, *99*, 95-99.

(37) Zhao, Y.; Truhlar, D. G. Density functionals with broad applicability in chemistry. *Acc. Chem. Res.* **2008**, *41*, 157-167.

(38) Zhao, Y.; Truhlar, D. G. A new local density functional for main-group thermochemistry, transition metal bonding, thermochemical kinetics, and noncovalent interactions. *J. Chem. Phys.* **2006**, *125*, 194101.

(39) Zhao, Y.; Truhlar, D. G. Density functional for spectroscopy: no long-range self-interaction error, good performance for Rydberg and charge-transfer states, and better performance on average than B3LYP for ground states. *J. Phys. Chem. A.* **2006**, *110*, 13126-13130.

(40) Zhao, Y.; Schultz, N. E.; Truhlar, D. G. Design of density functionals by combining the method of constraint satisfaction with parametrization for thermochemistry, thermochemical kinetics, and noncovalent interactions. *J. Chem. Theory Comput.* **2006**, *2*, 364-382.

(41) Weigend, F.; Furche, F.; Ahlrichs, R. Gaussian basis sets of quadruple zeta valence quality for atoms H–Kr. *J. Chem. Phys.* **2003**, *119*, 12753-12762.